Journal of Robotics and Control (JRC)
Volume 4, Issue 4, 2023
ISSN: 2715-5072, DOI: 10.18196/jrc.v4i4.19299

Analysis of ANN and Fuzzy Logic Dynamic Modelling to Control the Wrist Exoskeleton

Mohd Safirin Karis [1]*, Hyreil Anuar Kasdirin [2], Norafizah Abas [3], Wira Hidayat Mohd Saad [4], Muhammad Noorazlan Shah Zainudin [5], Nursabillillah Mohd Ali [6], Mohd Shahrieel Mohd Aras [7]
[1] Faculty of Electrical and Electronic Engineering Technology, Universiti Teknikal Malaysia Melaka, Ayer Keroh, Melaka, Malaysia
[2, 3, 6, 7] Faculty of Electrical Engineering, Universiti Teknikal Malaysia Melaka, Durian Tunggal, Melaka, Malaysia
[4,5] Faculty of Electronic and Computer Engineering, Universiti Teknikal Malaysia Melaka, Durian Tunggal, Melaka, Malaysia
Email: [1] safirin@utem.edu.my, [2] hyreil@utem.edu.my, [3] norafizahabas@utem.edu.my, [4] wira_yugi@utem.edu.my, [5] noorazlan@utem.edu.my, [6] nursabillilah@utem.edu.my, [7] shahrieel@utem.edu.my
*Corresponding Author

***Abstract*—Human intention has long been a primary emphasis in the field of electromyography (EMG) research. This being considered, the movement of the exoskeleton hand can be accurately predicted based on the user's preferences. The EMG is a nonlinear signal formed by muscle contractions as the human hand moves and easily captured noise signal from its surroundings. Due to this fact, this study aims to estimate wrist desired velocity based on EMG signals using ANN and FL mapping methods. The output was derived using EMG signals and wrist position were directly proportional to control wrist desired velocity. Ten male subjects, ranging in age from 21 to 40, supplied EMG signal data set used for estimating the output in single and double muscles experiments. To validate the performance, a physical model of an exoskeleton hand was created using Sim-mechanics program tool. The ANN used Levenberg training method with 1 hidden layer and 10 neurons, while FL used a triangular membership function to represent muscles contraction signals amplitude at different MVC levels for each wrist position. As a result, PID was substituted to compensate fluctuation of mapping outputs, resulting in a smoother signal reading while improving the estimation of wrist desired velocity performance. As a conclusion, ANN compensates for complex nonlinear input to estimate output, but it works best with large data sets. FL allowed designers to design rules based on their knowledge, but the system will struggle due to the large number of inputs. Based on the results achieved, FL was able to show a distinct separation of wrist desired velocity hand movement when compared to ANN for similar testing datasets due to the decision making based on rules setting setup by the designer.**

Keywords—Artificial Neural Network (ANN); Fuzzy Logic (FL); Exoskeleton Wrist Control; PID; Mapping Methods.

I. INTRODUCTION

Understanding the human motion intention has become a new era challenge for intelligent human–computer interaction. This subject has been substantially studied in all research on how to assist a person whose loss of limbs hinders physical functionality and movement, which severely lowers the quality of life. In the United States, 1.9 million persons lost a limb in 2012, with 41,000 of those cases affecting the upper limb [1]. Traumatic events, underlying medical diseases, comorbidities, or a genetic illness can all lead to upper limb insufficiency. Prosthetic fittings are available as the main form of functional support for the majority of acquired amputations and some congenital limb abnormalities. This device mostly required data captured from muscles contraction namely electromyography (EMG) signals which was used to analyze and capture the neuromuscular activation observed in the various muscles during different physical activities that contains the movement intention of the human body [2].

Surface EMG, also referred to as sEMG, is a common way to depict human intention. A bioelectric signal called surface electromyography (sEMG) is created when muscles are naturally activated by the nervous system [3]. The human body's intended movement is encoded in the sEMG through the mapping between muscle location and activation level. Controlling a myoelectric hand, an exoskeleton, and other devices are where it finds the most widespread application [4], [5]. The human hand, on the other hand, is a highly articulated joint with several degrees of mobility. Electromyography (EMG) recorded from extrinsic muscles in the forearm can be used as inputs to control a multi-degree of freedom (DoF) hand exoskeleton and prosthesis because the movement of the hand is directly supported by significant muscles contraction depending on the user's decision [6], [7], [8], [9].

Since the EMG signal was recorded while a person formed a hand movement, understanding that it naturally has a nonlinear structure is crucial. It is easily influenced by noises in its environment. The noises due to the type of electronic equipment, movement of electrodes and cables, movement of the subject during signal recording, artifacts, muscle fatigue, crosstalk and other physiological factors which need proper detection and processing of EMG signals with effective and advance methodologies may be a fundamental requirement for its applications in different control fields [10], [11], [12].

The primary objective of this paper was to propose mapping methods that enhanced the control of the wrist exoskeleton hand. For this purpose, the designer chose to analyze two approaches, namely Artificial Neural Network (ANN) and Fuzzy Logic (FL), utilizing EMG signals obtained from experimental results. FL was selected for its proficiency in handling nonlinear systems and adaptability to changes within a system, making it suitable for dynamic and

evolving situations. On the other hand, ANN was chosen for its capability to capture complex relationships between input and output data, allowing it to learn from examples and continuously adjust its internal parameters (weights) to improve performance over time. Considering these distinct advantages possessed by both mapping methods, the designer analyzed their potential in enhancing the control performance of the wrist desired velocity system.

In this paper, the designer addresses the research gap concerning the comparison analysis performance of two mapping methods: ANN and FL. The objective was to guide researchers in selecting the most suitable method by utilizing similar datasets. Furthermore, the results obtained from these mapping methods can be leveraged to improve the performance of the PID controller to model and control wrist exoskeleton hand movements.

This paper has been structured into four main sections: recent developments in EMG control methods, methodology, results, and conclusion. The "Recent Development of EMG Control Method" section explores various types of control strategies employed in the field. In the "Methodology" section, presented the testing methods used for system validation, including detailed procedures, processes, and settings for each approach. The "Results and Discussion" section analyzes the performance of the selected methods through single and double muscle experiments, with the inclusion of PID to complete the overall system testing. Finally, in the "Conclusion" section, summarize all the analyses and propose future research directions.

II. RECENT DEVELOPMENT OF EMG CONTROL METHOD

EMG-based human intention recognition has three main processing approaches. They are deep learning based method (DL), model based (MB) method and machine leaning (ML) based method, [13], [14] as shown in Table I. DL can be defined as finding a relationship between inputs and desired outputs using a neural network. With less requirement for feature engineering and kinematic modelling, this approach opens up more opportunities for fixing the initial problems with older approaches [15]. On the one hand, deep learning is data-driven, therefore performance increases with increased data [7]. Deep neural networks and augmented datasets can provide more stable, abstracted properties. However, this approach has a black box input-output relationship.

Several artificial intelligence systems transform input sets to output sets without considering muscle working formulation. In essence, a system was given a wide variety of inputs and related outputs using this technique. After training, the system should predict the continuous motion parameter from a random EMG signal. This approach is frequently used in continuous motion prediction using EMG. The neural network model, fuzzy approximation, Bayesian network, hidden Markov model, and Kalman filter may predict continuous human upper limb movements [16], [17], [18], [19].

Researchers frequently use the model-based approach to estimate joint angle, force, torque, and other continuous motion parameters. Because inputs and outputs are interrelated, model-based techniques construct a linear or nonlinear analytical relationship. The connection may additionally utilize unknown input features like wrist function, finger angle, and hand gesture to estimate the target output. These variables may initially be established through experimentation or by making some assumptions. The settings are then changed repeatedly until the desired version performance is attained. This approach can be expressed as a kinematic, dynamic, or musculoskeletal model depending on the intention identification purpose, which requires accurate representation of human limbs [14].

The method based on machine learning has been frequently used to identify the patterns present in EMG signals. Usually, researchers use this strategy to classify limb gestures. Pre-processing, feature extraction and selection, and machine learning comprise the machine learning-based strategy, according to Simão et al. [13]. It systematically mapped input to output, categorizing the output required accuracy and efficiency. Thus, such reconstruction methods may project EMG data into a discriminant space with exceptional movements. It is advantageous to learn about the new input data structure because it might enhance discrimination to enhance overall performance. Machine learning (ML) computing can extract the specified features from the targeted data and quantify them for model training using supervised learning including K-Nearest Neighbour (KNN) Linear Discriminant Analysis (LDA) Support Vector Machine (SVM) and Artificial Neural Networks (ANN) [20], [21], [22], [23], [24], [25], [26].

Since the discovery of feature extraction methodology, the development of EMG processing methodology has consistently been emphasized aspect. Using data from Table I, three techniques were identified and tallied for use from 2012 through 2023. Most researchers are now concentrating more on employing machine learning techniques as the earlier years of 2012 to 2019 get underway. The pattern recognition classifier, pre-processing, feature extraction, machine learning, and final output result are all covered by this method. Machine learning was successful in covering hand and wrist angle movement, which added a variety of novelties to the EMG area, on the upper limb body part. However, in this within range of years there has been exploration on the other two methods which are model based and deep learning done by Kawase et al. [27], Songyuan Zhang et al. [16] and Du Jiang [19]. All these researchers explore a novelty on hand and wrist movement activities. As additional research focused more on model-based and deep learning got involved, most researchers began to expand their control approach tactics starting in the year 2020 and above. Researchers are adapting more research on hand and wrist movement as they stress this strategy in their experimental designs. However, other researchers have continued to make advances in studying this machine learning technique up to this point.

The classification of bio-signal using traditional machine learning models relies on handcrafted features that have been painstakingly picked and developed. EMG signal-based limb motion recognition, robot control, rehabilitation, and clinical research have used supervised ML algorithms [28].

Numerous factors, including EMG recording techniques (such as different electrodes, electrode placement locations on the body surface, or recording devices), bio-variability (age and body mass index), environmental factor (room temperature), electrical power line noise, and motion artefact, affect the accuracy of feature extraction from the EMG signals. These effects decrease system robustness and recognition accuracy requiring complicated signal processing [29]. However, in order to optimize estimation performance, machine learning algorithms need a large amount of datasets [30].

TABLE I. CHRONOLOGY DEVELOPMENT OF EMG PROCESSING METHOD

No	Author	Year	Control Method			Body Part
			ML	*MB*	*DL*	
1	Pang et al. [37]	2012	■			Hand
2	Loconsole et al. [38]	2013	■			Hand
3	Ngeo et al. [39]	2013	■			Hand
4	Kawase et al. [27]	2014		■		Wrist
5	Li et al. [40]	2014	■			Wrist
6	Kirchner et al. [41]	2014	■			Wrist
7	Leonardis et al. [42]	2015	■			Hand
8	Songyuan et al. [16]	2016			■	Wrist
9	Accogli et al. [43]	2017	■			Wrist
10	Lu et al. [44]	2017	■			Hand
11	Yun et al. [45]	2017	■			Hand
12	Irastorza-Landa et al. [46]	2017	■			Wrist
13	E. Kilic et al [32]	2017	■			Wrist
13	Zeng et al. [47]	2018	■			Hand
14	Jana et al. [48]	2019	■			Hand
15	Lei et al. [17]	2019	■			Wrist
16	Lu et al. [49]	2019	■			Hand
17	Secciani et al. [50]	2019	■			Hand
18	Burns et al. [51]	2019	■			Hand
19	Du Jiang [19]	2019		■		Hand
20	Chenyun Dai et al. [52]	2020	■			Hand
21	Qin Zhang et al. [53]	2020		■		Hand
22	Yihui Zhao et al.[54]	2020		■		Wrist
23	Itzel Jared et al. [55]	2020		■		Hand
24	Tamas Kapelner et al. [56]	2020		■		Wrist
25	Davide Piovesan et al. [57]	2020		■		Hand
26	Tianao Cao et al. [58]	2020	■			Wrist
27	Longbin et al. [59]	2020			■	Wrist
28	Xiao et al.[60]	2021	■			Hand
29	Xie et al. [61]	2021		■		Hand
30	M. Mukhtar et al. [62]	2021		■		Hand
31	Davis A. et al. [63]	2021		■		Wrist
32	Nguiadem et al. [64]	2021		■		Wrist
33	Nicole J. et al. [65]	2021			■	Wrist
34	Cries Avian et al.[66]	2022		■		Hand
35	Maurício et al [33]	2022		■		Hand
36	Mahsa [34]	2022	■			Hand
37	Ravi Suppiah et al [35]	2022			■	Hand
38	Yihui Zhao et al [12]	2023		■		Wrist
39	Sibo Yang et al [67]	2023	■			Hand
40	Yassine et al [68]	2023		■		Hand
41	Jianan Li et al [69]	2023	■			Hand/ wrist
42	Markus et al [24]	2023	■			Hand/ wrist

ANN mimic human behavior, allowing laptops to recognize patterns and tackle basic AI, deep learning, and machine learning challenges. B. Chen et al. and L. Meng et al. found that ANN can extract features from data samples for machine learning computing [25], [26]. It simulates a human brain's neuron network so the computer can think and decide like a person. ANNs may study from times, replicate arbitrary non-linear input functions, and have a substantially parallel and normal shape, making them ideal for pattern categorization [31]. An ANN is typically trained or fed enormous amounts of information, which includes training, providing input, and instructing the network as to what the output should be. However, ANN is a data-driven technique because the accuracy of the output increased as more data were fed into the training network [7].

The trends of introducing FL in a control method also increase as E. Kilic et. al, 2017 [32], Du Jiang et. al, 2019 [19], Maurício Cagliari Tosin et. Al, 2022 [33], Mahsa Barfi et. Al, 2022 [34], and Ravi Suppiah et. Al, 2022 [35] used FL in their decision making output process FL allows many inputs and interprets them based on human expertise. The recorded EMG signals from the forearm muscles in charge of hand and wrist movements are the inputs to the FL. The FL output might be the wrist's assistive torque or desired angular velocity because EMG signals directly connect to muscle activation as higher muscle activation levels produce more force. Since the admittance controller, one of the most widely used control theories for robotic rehabilitation systems, accepts force as an input and allows velocity as an output, joint angle and angular velocity were chosen as FL outputs in most studies [36].

III. METHODOLOGY

A. Mechanical Hand Design

The exoskeleton was designed to mimic the human hand. From ten male subjects ages from 21 to 40 years old, all the anthropometric hand measurement were taken.

Fig. 1 shows completed exoskeleton hand designed model. For this paper, one degrees of freedom (DoF) of the wrist joint angle position has been highlighted in this exoskeleton hand designed covered three types of gestures: hand gripping at -45°, 0°, and 45° as shown in Fig. 2. Since the wrist exoskeleton hand can be moved to achieve wrist velocity, it is completely actuated.

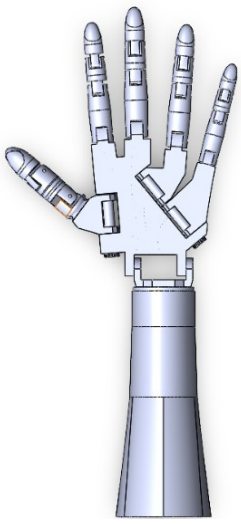

Fig. 1. Exoskeleton prototype design

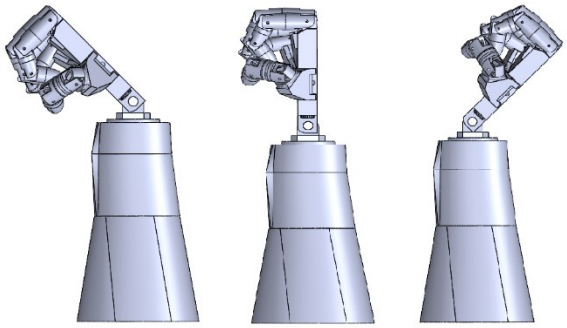

(a) (b) (c)

Fig. 2. Solidwork 3D Hand Design (a) Flexion Position, (b) Neutral Position, (c) Extension Position [70]

B. EMG Data Collection

Ten male subjects signed the researcher's consent form to undertake the hand grip pattern experiment at varying wrist joint angles. The experiment began after the subjects were fully briefed. Each experiment was repeated three times [71]. This experiment used a Hand Dynamometer, LabQuest Mini data acquisitions, Vernier EMG sensors, a personal computer with Logger Lite data-collection software, Stopwatch, Protector, and Kendall5400 diagnostic tab electrodes. All experiments were approved by the University Ethical Committee or Centre for Research and Innovation Management (CRIM) at University Technical Malaysia Melaka (UTeM) Malaysia.

The Flexor Carpi Radialis (FCR) and Extensor Carpi Radialis Longus (ECRL) EMG signal values have been employed in this research to represent each wrist joint angle movement [72], [32], [73]. The electrode was placed right on top of muscle belly to ensure the signals response will represent the actual readings of muscle contraction. All of the subjects were in good health with non-neurological diseases and used their dominant hand for data collection. From one task to another, the subjects will take 10s rests to ensure the effects of muscle fatigue can be reduced. The medial epicondyle has been used to locate the muscles and the palpate Scaphoid technique has been employed to determine the wrist movement [74], [75]. Table II shows the testing procedure on specifying the muscle location done in the experimental procedure.

TABLE II. MUSCLE IDENTIFICATION TEST AND ITS LOCATION FOR ELECTRODE PLACEMENT

No	Muscle	Test	Location
1	Flexor Carpi Radialis (FCR)	The wrist is flexed against resistance.	Three or four fingerbreadths away from the midpoint of a line connecting the medial epicondyle and biceps tendon.
2	Extensor Carpi Radialis Longus (ECRL)	The wrist is extended and abducted with the forearm pronated.	Two fingerbreadths away from lateral epicondyle.

Fig. 3 illustrates how experimental procedures conducted. The maximal force (MVC) of the hand grasp is a measurement of the subject's strongest voluntary contraction Electrode patches are put to the top of the abdominal muscles of FCR and ECRL. For five seconds, the samples were instructed to hold the hand dynamometer while using different hand grip strengths (20, 40, 60, 80, and 100% MVC) [71]. Each grip includes a two-second rest interval. The retrieved raw EMG signals were recorded using the Logger Lite programme.

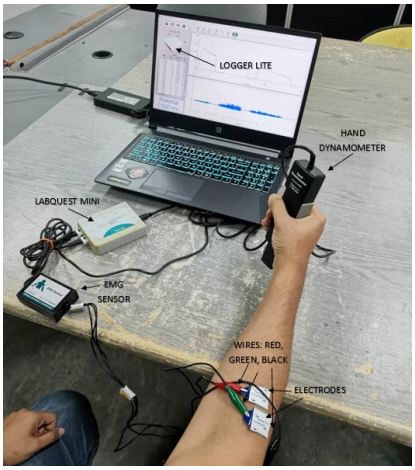

Fig. 3. Experimental set-up [70]

C. EMG Signal Processing

This paper adapted time-domain-based features using Waveform Length (WL) approach [76], [77]. The sampling frequency was chosen at 1 kHz to suit the EMG signals range (2Hz – 2kHz). The segmentation of input data was reduced at 50% analysis window increment. A second-order band-pass Butterworth filter was used for this experimental procedure [78]. The maximum voluntary contraction (MVC), which was uniquely recorded from each subject, has been used to standardise EMG measurement values. This method scales the measurement between 0 to 1 and most used normalization techniques in MVC-normalization [79], [80]

D. Mapping Process

Modelling establishes a link between all usage parameters. It establishes a link between inputs and outputs in sequence. This modelling constructs a correct transfer function to describe system performance and measured efficacy of selected modelling approach. Modelling, sometimes called mapping, is a data groping representation of numerous types of group design. Since this paper recommended employing two mapping methods, ANN and FL were tested using the same data set to ensure a comparable output result.

ANN and FL are among the preferable methods used by other researchers to generate an output result if the non-linear input was given. Using the advantages of both methods presents, they have been chosen to be a part of mapping method of EMG input and wrist position to predict the estimated wrist desired velocity output. While ANN excels in handling nonlinear inputs, its performance may suffer when dealing with small input datasets that cannot effectively create a network. Similarly, FL can handle nonlinear inputs and produce estimated results, but it requires clearly defined ranges of input data to avoid incorrect estimations and prevent significant errors.

1) Method 1: Dynamic Modelling of Wrist Movement Using Artificial Neural Network (ANN)

Traditional feedforward neural networks are one-way mappings from input to output and do not use input signal dependency over time series. Depending on application complexity, neural networks can approximate nonlinear functions using adaptive weights on different layers [81]. Numerous related research papers have shown how good neural networks are in recognizing EMG patterns [82]. Francisco et al., 2020, used a regression algorithm with neural networks to create a multiclass categorization model to control a robotic system with three degrees of freedom of the anthropomorphic type that can accurately remote the robot arm to predetermined positions in a state machine [83].

ANN show promise performance for identifying motion-based bio signal patterns and can capture system nonlinearity and have a low computational burden [15], [84]. ANN approach requires training a network using input data to represent the system. Three sets of data were collected from one sample. Two data sets were used for training and one for testing to complete the process. The WL feature extraction algorithm has been used to extract the features produced by extensor and flexor muscles of the EMG signal. EMG_F (EMG value when the wrist was in flexion position), EMG_E (EMG value while the wrist was in extension position), and wrist joint angle position are the three types of inputs for single muscle response have been used to estimate the desired wrist velocity output. The design architecture for single muscle is shown in Fig. 4(a) below. Fig. 4(b) shows an ANN designed architecture inputs for double muscles experimental procedure consists of FCR and ECRL muscles to estimate the output for wrist desired velocity.

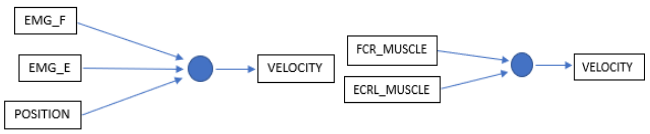

Fig. 4. (a) Design ANN architecture for single muscle experimental procedure. (b) Design ANN architecture for double muscle experimental procedure.

Single muscle approach shown in Fig. 5(a) and (b) compares signals at 20% MVC, 60% MVC, and 100% MVC Level between EMG_F and EMG_E. MVC at the same level should result in no wrist movement. The MVC's other value levels should adhere to the one that is higher than the others.

By realizing through this signal comparison experiment, the wrist desired velocity movement of can be estimated. However, signals from both graphs fluctuate, which may create wrist result velocity inaccuracy.

For double muscle approach, 2 input signals have been sampled simultaneously from FCR and ECRL muscle responses shown in Fig. 5 (c) and 5 (d). The desired wrist velocity was the anticipated output from the ANN trained model. The wrist desired velocity output testing was estimated at 20% MVC and at 60% MVC level. At 20% MVC output, the signal generated showed a clear fluctuation at 75s and below where the state was at neutral wrist position. The signal stabilises about 75s–150s. However, at 150s and above, the signal response fluctuated in extension wrist position. In the 60% MVC level, the signal produced a more stable output result as it fluctuates only on each stage.

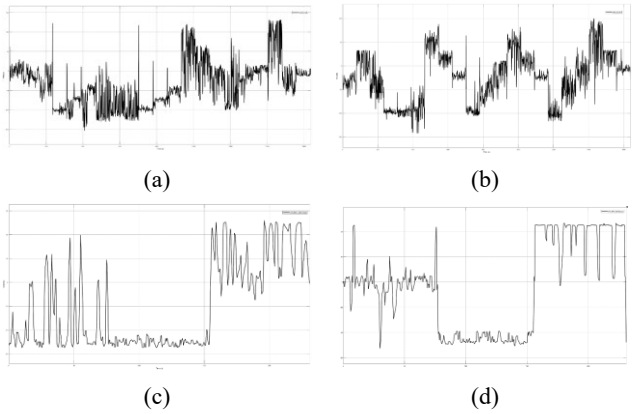

Fig. 5. (a) single muscle response for FCR, (b) single muscle response for ECRL, (c) double muscles response at 20% MVC level, (d) double muscles response at 60% MVC level

2) Method 2: Dynamic Modelling of Wrist Movement Using Fuzzy Logic (FL)

Fuzzification, rules (knowledge), an inference system, and defuzzification are the four fundamental components of FL. Fuzzification is used to transform actual data into a membership function. To make decisions, rules are formed based on knowledge. The inference system is a decision-making system that employs knowledge-based rules. Defuzzification converts an inference system's conclusion to actual data or real-world data so that it can interact with the actual system. Fig. 6 depicts a FL configuration concept.

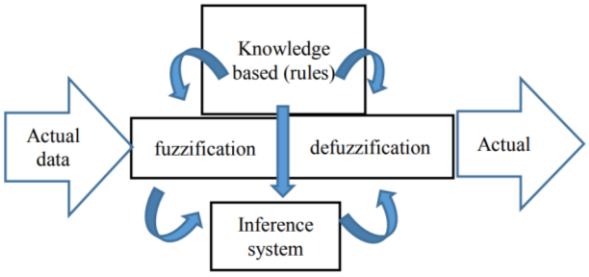

Fig. 6. Basic configuration of FLC concept [85]

FL studies human thought processes. It offers a straightforward way of drawing a firm conclusion from ambiguous and unpredictable data. FL has many advantages because of its inherent efficacy. It doesn't need inputs that are precise and noise-free. Even with a broken feedback sensor, it works securely. Any sensor data that gives a vague sense of how well a system is doing is sufficient. The rule-based procedure allows for the consideration of any multiple inputs and the handling of any number of outputs [86]. According to Momen Kamal Tageldeen et al. 2017, FL can include expert knowledge into controller design, reducing uncertainty [87].

Fig. 7 shows a FL architecture for single muscle and double muscle approaches. As for Fig. 6 (a), single muscles architecture of EMG signals from the forearm muscles and wrist joint angle position were recorded by the FL's three inputs while Fig. 7 (b) designed architecture specified for

double muscles as two inputs have recorded EMG signals from two forearm muscles. As one of the most popular control theories for exoskeleton hand systems, the desired velocity of the hand wrist has been selected as the FL's output [59]. The activation rate for extensor and flexor muscles of the EMG signal has been continuously assessed using WL feature extraction algorithms. To match up similar data sets utilized for both mapping methods, the data set used for testing in the ANN method will be used to complete the FL procedure.

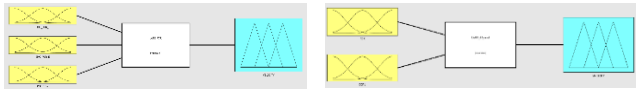

(a) (b)

Fig. 7. (a) FL design for single muscle, (b) FL design for double muscles [70]

Fig. 8 (a), (b), (c), (d) and (e) shows that FL fuzzyifies input variables for both approaches before generating the rule table using membership functions. For single muscle approach, shown in Fig. 8 (a), (b), and (c) inputs indicated three triangular-shaped membership functions used to fuzzify EMG signals and two trapezoidal-shaped membership functions used to fuzzify wrist joint angle position at 20%, 60%, and 100% MVC level. EMG_F and EMG_E were used to analyze FCR and ECRL muscles input. EMG signals have been classified as SMALL (S), MEDIUM (M), and HIGH (H). As for double muscle approach shown in Fig. 8 (d) and (e), FCR and ECRL muscles have been using similar concepts of triangular membership functions to classify its signals. FL outputs wrist desired velocity used five triangle membership functions was categorized as FH (flexion high: 100°/s), FM (flexion medium: 50°/s), Z (zero velocity: 0°/s), EM (extension medium: 50°/s), and EH (extension high: 100°/s) in the output Fig. 8 (f). Input triangular membership functions are defined based on the testing data after passing through the feature extraction process. For input, the highest and lowest data numbers were taken from their own group dataset to form this triangular membership function.

Table III above displayed 15 IF-THEN rule statements. EMG_F and EMG_E are signals generated during wrist joint angle for flexion and extension. According to the first three fundamental criteria listed in Table III, both flexion and extension actions should result in zero wrist desired velocity when both signals have been in similar level. The following six rules investigated how various EMG signal excitations affected predictions of the wrist-desired velocity. To complete the fifteen criteria, guidelines limited the device's wrist joint angle (Θ) and added wrist velocity (Θ/s) safety measures. The 15 linguistic statements in the rule table are all combined to form a Mamdani-style fuzzy inference method that maps the inputs to the output.

Table IV above shows 9 IF-THEN rule statements. FCR muscle signal level was highest during wrist flexion, hence the parameter data was captured, while ECRL muscle signal level was highest during wrist extension. The wrist velocity has been suspected to produce zero state if the EMG signals generated by flexion and extension actions of wrist movement have similar value. FM is made if FCR is more than ECRL, and EM if ECRL is greater. FH was made when FCR was much greater than ECRL, and EH was produced when ECRL was much more than FCR. Comparing the EMG signal strength allowed researchers to predict the movement of wrist position.

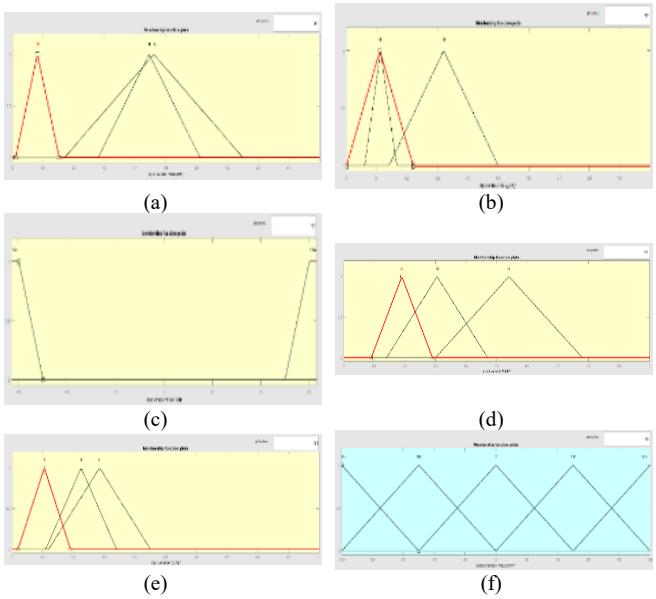

(a) (b) (c) (d) (e) (f)

Fig. 8. (a) Function of triangular-shaped membership used for EMG signal (EMG_F), (b) Function of triangular-shaped membership used for EMG signal (EMG_E), (c) Function of trapezoidal-shaped membership used for wrist joint angle (POSITION), (d) Function of triangular-shaped membership used for FCR Muscle, (e) Function of triangular-shaped membership used for ECRL Muscle, (f) Function for triangular membership used for the desired wrist velocity [70].

TABLE III. IF-THEN RULE STATEMENTS [32]

No		EMG_F		EMG_E		(Θ)		(Θ/s)
1	if	S		S			=	Z
2	if	M		M			=	Z
3	if	H		H			=	Z
4	if	M	&	S	&	not Flim	=	FM
5	if	H	&	M	&	not Flim	=	FM
6	if	H	&	S	&	not Flim	=	FH
7	if	S	&	M	&	not Elim	=	EM
8	if	M	&	H	&	not Elim	=	EM
9	if	S	&	H	&	not Elim	=	EH
10	if	M	&	S	&	Flim	=	Z
11	if	H	&	M	&	Flim	=	Z
12	if	H	&	S	&	Flim	=	Z
13	if	S	&	M	&	Elim	=	Z
14	if	M	&	H	&	Elim	=	Z
15	if	S	&	H	&	Elim	=	Z

TABLE IV. IF-THEN RULE STATEMENTS [70]

No		FCR Muscle		ECRL Muscle		(Θ/s)
1	if	S	&	S	then	Z
2	if	M	&	M	then	Z
3	if	H	&	H	then	Z
4	if	M	&	S	then	FM
5	if	H	&	M	then	FM
6	if	H	&	S	then	FH
7	if	S	&	M	then	EM
8	if	M	&	H	then	EM
9	if	S	&	H	then	EH

Fig. 9 (a) and (b) shows the FL signal output of desired wrist velocity for single muscle approach. Based on these

output result, identical levels of MVC values should generate a velocity value of zero. As the input signal from EMG_F became greater than EMG_E, the velocity of the hand shifted from extension to flexion and vice versa. The wrist's desired velocity amplitude changes when tested data is compared to larger or smaller values. When the wrist is in flexion, the FCR muscle is stimulated more aggressively, while in extension, the ECRL responds more aggressively. Even when in the opposite posture, both muscles produced EMG output signal voltages, but the reading was lower. In contrast, both EMG signal muscles should result in equally stimulated voltages of signal strength from both muscles when the wrist is in a neutral position.

In Fig 9 (c) and (d) shows wrist desired velocity fuzzy output results for double muscle approach. At signal level 20% MVC, the estimated data division readings for each wrist joint angle position overlap, resulting in an unstable desired wrist velocity output. At signal level of 60% MVC, figure shows a considerable desired wrist velocity fuzzy output result, as each component of wrist position can be easily recognized. This contributes during feature extraction, the EMG signal value excitation begins to show its great group uniqueness, thus making the wrist desired velocity output data easier to understand.

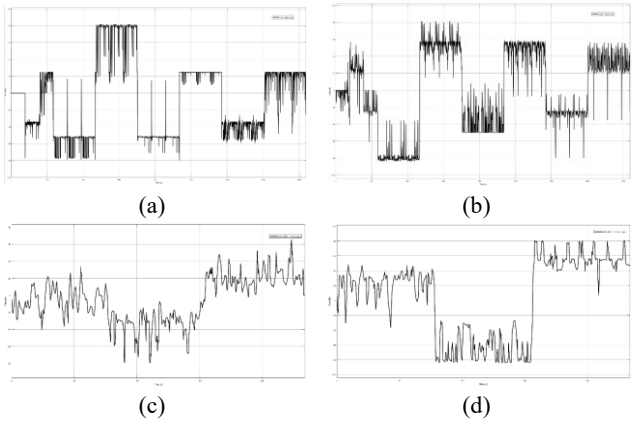

Fig. 9. (a) single muscle response for FCR, (b) single muscle response for ECRL, (c) double muscles response at 20% MVC level, (d) double muscles response at 60% MVC level.

E. PID Control

Proportional integral derivative (PID) controllers use a control loop feedback technique to manage process variables The steady state error for monitoring a step input signal is one of the integral terms that is eliminated or reduced. In actual implementation, the integral term is usually limited by some hounds. PID's primary purpose is to balance out the fluctuating output mapping signal, which results in more stable continuous output control for the exoskeleton hand. In this paper, metaheuristic algorithm has been applied to obtain the value for KP, KI and KD [88].

Tuning the parameters (KP, KI, and KD) of a PID controller using metaheuristic methods involves using trial and error method to find the optimal values that result in the best control performance for a given system. Metaheuristic methods are global optimization algorithms that explore the parameter space efficiently, even for non-linear and complex systems. The main objective using PID in this system was to ensure the movement of the hand fluently move from one state to the other. The challenge faced in this nonlinear given input coming from mapping method decision making are fluctuated occurred in each stage. The best parameter for PID chosen must be able to smoothen the ripple produce thus help to compensate the modelling of wrist movement. The value for KP = 3.97 x 10^{-9}, KI = 0.11 x 10^{0} and KD = 1.44 x 10^{-6}[70].

IV. Results and Discussions

The following step involves importing the SolidWorks file into MATLAB environment. At this point, a controller for the desired wrist velocity can be built using any Simulink feature, such as ANN and PID or FL and PID [87]. PID has been utilized to control the output from ANN and FL to estimate the desired wrist velocity. The PID output was preferable to produce a slower response that does not immediately follow the changes made-up by decision making process in each stage within specific wrist position. Similar plants have been used for both method approaches. The finished SimMechanics testing system for physically modelled exoskeleton hands is shown in Fig. 10 and 11.

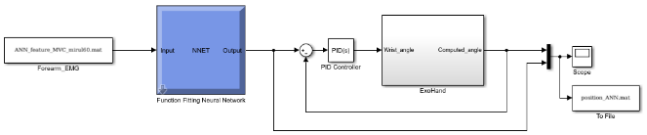

Fig. 10. Full system of exoskeleton hand for wrist movement with ANN and PID controller

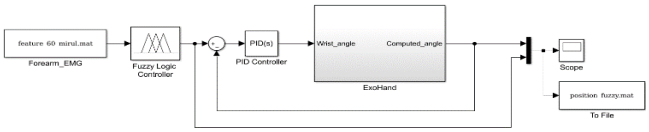

Fig. 11. Full system of exoskeleton hand for wrist movement with FL and PID controller [70].

A. Analysis of Designed Performance using PID

ANN and PID controller have been applied for the exoskeleton hand system to predict the wrist desired velocity. Fig. 12 (a) and (b) shows wrist desires velocity at various MVC levels for single muscle response. The red line graph in both figures represents the ANN decision making based on the testing data given to the training block, while the blue line graph represents the exoskeleton desired wrist velocity result after passing through the PID controller block. FCR muscle response result in Fig. 12 (a) showed overshoot from 600s to 800s and undershoot at 1400s. ECRL muscle response figure shows overshoot cases at 600s to 800s and undershoot cases at 1400s to 1600s illustrated in Fig. 12 (b). PID is one controller mechanism used to compensate for ANN decision making output fluctuation. As seen in both blue graphs in both ANN Fig. 12 (a) and (b), PID smoothed the instability output for the desired wrist velocity and wrist movement.

Fig. 12 (c) and (d) demonstrates the FL and PID controller and FL output result based on the performance of a single muscle affected on desired wrist required velocity of the exoskeleton hand system. The dynamic model of the system has been initially implemented using FL. However, when the exoskeleton hand model was fed the output from the FL mapping method, the wrist velocity output result was

unstable. Both graphs' red lines were created by FL's decision-making process. As seen in Fig. 12 (c) for FCR muscle response, overshoot occurred between 200s and 400s and undershoot from 1400s to 1600s. ECRL muscle response in Fig. 12 (d) showed overshoot at 700s to 900s and undershoot at 900s to 1100s. PID controllers have been used to stabilise anticipated output values due to FL instability. The blue line graph in each figure showed the exoskeleton hand output after the PID controller was built. The results smoothed the exoskeleton hand's wrist velocity by adjusting for FL mapping process irregularities.

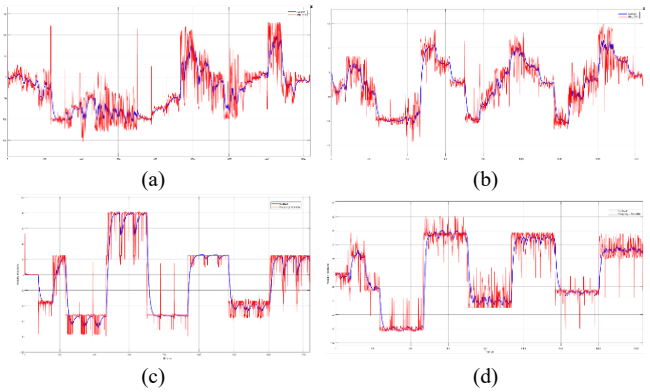

Fig. 12. (a) ANN and PID single muscle response for FCR, (b) ANN and PID single muscle response for ECRL, (c) Fuzzy and PID single muscle response for FCR, (d) Fuzzy and PID single muscle response for ECRL [70]

Fig. 13 (a) and (b) shows double muscle response at 20% and 60% MVC using ANN and PID approach to determine exoskeleton hand system wrist desired velocity output graph. This exoskeleton hand technology uses ANN as its mapping method to generate the estimated output result. The red line graph generated by the ANN mapping procedure was displayed in both figures show a small fluctuation in their plotting. The ANN output exhibited almost imperceptible differences in pattern from the preceding state at 20% MVC shown level in Fig. 13 (a). However, after 150s, the state begins to differentiate. The red line graph revealed a notable pattern in each stage's desired wrist velocity condition at 60% MVC level shown in Fig. 13 (b). Every red line graph in both figures showed exoskeleton wrist velocity variability that needed adjustment. To improve exoskeleton hand system performance, PID controllers have been adopted. By using PID, the blue graph appeared in both figures. The purpose of PID was to eliminate ripple from the ANN decision-making process and increase the stability of the output reading. The pattern graph in the earlier stage, however, still introduces a fluctuation at a 20% MVC figure and generates nearly identical pattern graphs at various stage levels. The pattern was more noticeable at 150s and above. For 60% MVC level, the blue line graph pattern from each stage was tuned and clearly recognised.

Fig. 13 (c) and (d) demonstrates the intended wrist velocity output of the FL and PID controller and FL based on two muscles for exoskeleton hand system. FL has been chosen as the mapping technique for the exoskeleton hand system. The selected method compared measurement data from each muscle's excitation group to predict desired wrist velocity. As shown in Fig. 13 (c) and (d), a red line graph illustrating a fluctuation of fuzzily produced outcomes. The pattern in each wrist's desired velocity was related to the creation of EMG signals for both graphs. At 20% MVC level shown in Fig. 13 (c), the pattern generations were not evident since the signals value provided closer range separation, but in Fig. 13 (d) at 60% MVC level graph, the signals value produced bigger range separation. PID has been used as the controller to account for the fluctuations caused by the output of FL. The blue line graph in both pictures was created using a PID controller to smooth out the volatility caused by the FL decision-making process. This led to the production of separate wrist desired velocity output outcomes at different wrist joint angle positions for the exoskeleton hand system.

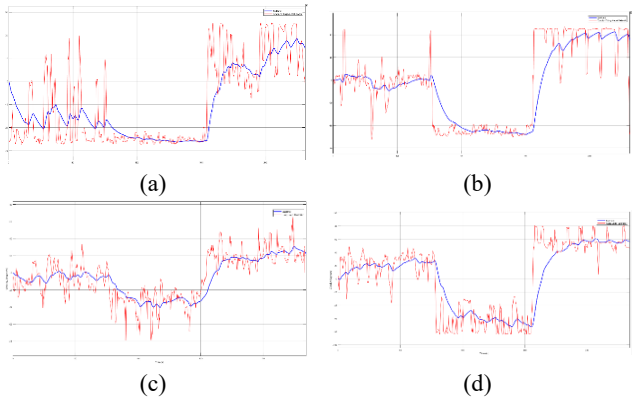

Fig. 13. (a) ANN and PID double muscles response for FCR and ECRL at 20% MVC, (b) ANN and PID double muscles response for FCR and ECRL at 60% MVC, (c) Fuzzy and PID double muscles response for FCR and ECRL at 20% MVC, (d) Fuzzy and PID double muscles response for FCR and ECRL at 60% MVC [70]

The accuracy results of both ANN and FL were directly compared, revealing that FL produced estimated outputs closer to the actual values. During the double muscle analysis comparison at 20% MVC and 60% MVC for ANN mapping output (Fig. 13 (a)), the actual output at 20% MVC was expected to be 0° (neutral), -30° (flexion), and 30° (extension). However, the estimated result showed oscillation at neutral, -30° at flexion, and 30° fluctuation at extension, indicating erroneous estimations that led to incorrect redirection of wrist movement. In contrast, the estimation results obtained by Fuzzy Logic clearly fluctuated around the real output for both 20% MVC and 60% MVC (Fig. 13(c) and Fig. 13 (d)). Although some minor variations occurred at the earlier stage of fuzzy output at the neutral position due to FL's decision-making process, it effectively distinguished each wrist position at every level. Regarding stability, in the same Fig. 13 (a), ANN produced unstable output results, particularly evident at the 20% MVC neutral state. Heavy fluctuations persisted even after PID attempted to stabilize the mapping process. The same situation occurred when examining ANN output at the 20% MVC extension state. In direct comparison to FL output at the 20% MVC neutral and extension states, the fluctuation range was significantly smaller than that produced by ANN results, demonstrating that FL and PID output yielded more stable results compared to ANN and PID.

During the experiment, one of the difficulties encountered was the movement of electrodes and cables. For the experiment, three electrodes were required to represent one muscle signal. Two electrodes were positioned side by side

to measure the voltage of the EMG signals, representing the positive and negative channels, while one electrode was placed on the bony region as the ground reference. However, as the wrist moved from one position to another, the electrodes tended to pull away from their original positions. To address this issue, wireless data transfer was considered the best solution. By employing wireless data transfer, the need for wires around the entire hand during the experiment was eliminated, allowing users to reduce noise interference caused by the wires.

In the discussion, it was highlighted that future research could be enhanced by choosing an appropriate mapping approach. Furthermore, each mapping method's estimation may incorporate different types of controllers to replace PID and reduce output fluctuations resulting from decision-making procedures. The implications of this study extend to prosthetic hand control, benefiting both stroke patients and amputees who have lost a hand. Additionally, beyond using EMG signals and joint angle to predict wrist desired velocity, the relationship between EMG signals and wrist joint angle could also be leveraged to predict force, such as hand grasp force and finger pinches.

V. CONCLUSIONS

Wrist hand position movement has become an integral component of human intentions in daily activities. Realizing the significance of this component, it is essential to emphasize the use of this wrist desired velocity estimation that follows the user's motion intention as employed in this paper, where it is also utilized for exoskeleton hand and other rehabilitation applications. The assessment of wrist desired velocity for the exoskeleton hand system can also be predicted using the relationship between wrist joint angle and EMG signals excitation. WL was chosen for feature extraction because it has a lower standard deviation compared to RMS, MAV, IEMG, and ZC [89]. Analyzing these standard deviation values has improved the tabulation of nearby data to determine the appropriate wrist velocity before mapping [90].

ANN can interpret unstructured data, but fuzzy systems are better at representing it [19]. For the whole exoskeleton hand system, ANN needs a training and testing data set. On the other hand, FL offered the freedom to create the exoskeleton hand system based on their own logic control. However, analyzing the performance of ANN and FL as dynamic models of the system allowed the researcher to build and choose the best approach for exoskeleton hand system applications. FL outperformed ANN in getting wrist desired velocity output for both approaches. Even though the wrist desired velocity fluctuated at each stage, the tabulated output data can easily distinguish belongings to each group. PID has been selected as the controller strategy to be applied in this paper. It can be applied to control the fluctuation caused by the mapping process chosen due to its simplicity and dependability in industrial applications.

Throughout the study, addressing the challenge of output fluctuation during the mapping process was a prominent concern. Estimating the output by mapping a nonlinear input signal required a thorough analysis of the produced errors. The research gap aimed to obtain estimation results of wrist desired velocity, which could assist in making informed decisions about selecting the optimal mapping method between ANN and FL, particularly when dealing with similar datasets. The careful choice of mapping method held critical importance in ensuring accurate modeling of wrist exoskeleton movement. Furthermore, the potential applications of this research extended to prosthetic hands and other rehabilitation devices, depending on the system's adaptability, thus contributing to enhancing the quality of life for users.

In addition, careful consideration was given to selecting appropriate PID parameters to effectively compensate for the fluctuations introduced by both mapping methods employed in this study. To achieve better outcomes, a potential improvement involves testing other mapping methods with higher accuracy than the ones used in this research. Additionally, applying an optimization approach to determine the best values for smoothing out any introduced ripples could lead to further enhancements.

ACKNOWLEDGMENT

The authors would like to thank the Ministry of Higher Education Malaysia for the financial support. The project is funded under Fundamental Research Grant Support. No (Ref: FRGS/1/2021/TK0/UTEM/02/54). The authors also want to thank Universiti Teknikal Malaysia Melaka for all the support.

REFERENCES

[1] K. Ziegler-Graham, E. J. MacKenzie, P. L. Ephraim, T. G. Travison, and R. Brookmeyer, “Estimating the Prevalence of Limb Loss in the United States: 2005 to 2050,” *Arch. Phys. Med. Rehabil.*, vol. 89, no. 3, pp. 422–429, 2008, doi: 10.1016/j.apmr.2007.11.005.

[2] R. Suppiah, A. Sharma, N. Kim, K. Abidi, and A. Alkaff, "An Electromyography-aided Robotics Hand for Rehabilitation – A Proof-of-Concept Study," *2020 IEEE Region 10 Conference (TENCON)*, pp. 361-366, 2020, doi: 10.1109/TENCON50793.2020.9293940.

[3] J. Vredenbregt and G. Rau, “Surface Electromyography in Relation to Force, Muscle Length and Endurance,” *New Concepts Mot. Unit, Neuromuscul. Disord. Electromyogr. Kinesiol.*, vol. 1, pp. 607–622, 2015, doi: 10.1159/000394062.

[4] C. J. D. Luca, “The use of Surface Electromyography in Biomechanics,” *J. Appl. Biomech.*, vol. 13, no. 2, pp. 135–163, 1997.

[5] K. Kiguchi and Y. Hayashi, “An EMG-based control for an upper-limb power-assist exoskeleton robot,” *IEEE Trans. Syst. Man, Cybern. Part B Cybern.*, vol. 42, no. 4, pp. 1064–1071, 2012, doi: 10.1109/TSMCB.2012.2185843.

[6] K. Gui, U. X. Tan, H. Liu, and D. Zhang, “Electromyography-Driven Progressive Assist-as-Needed Control for Lower Limb Exoskeleton,” *IEEE Trans. Med. Robot. Bionics*, vol. 2, no. 1, pp. 50–58, 2020, doi: 10.1109/TMRB.2020.2970222.

[7] T. Bao, S. A. R. Zaidi, S. Xie, P. Yang, and Z. Q. Zhang, “A CNN-LSTM Hybrid Model for Wrist Kinematics Estimation Using Surface Electromyography,” *IEEE Trans. Instrum. Meas.*, vol. 70, 2021, doi: 10.1109/TIM.2020.3036654.

[8] Y. Zhao *et al.*, “Adaptive Cooperative Control Strategy for a Wrist Exoskeleton Using Model-Based Joint Impedance Estimation,” *IEEE/ASME Trans. Mechatronics*, vol. 28, no. 2, pp. 748–757, 2022, doi: 10.1109/TMECH.2022.3211671.

[9] N. Lotti *et al.*, “Myoelectric or Force Control? A Comparative Study on a Soft Arm Exosuit,” *IEEE Trans. Robot.*, vol. 38, no. 3, pp. 1363–1379, 2022, doi: 10.1109/TRO.2021.3137748.

[10] A. Sultana, F. Ahmed, and M. S. Alam, “A systematic review on surface electromyography-based classification system for identifying hand and finger movements,” *Healthc. Anal.*, vol. 3, no. October 2022, p. 100126, 2023, doi: 10.1016/j.health.2022.100126.

[11] J. Fu, R. Choudhury, S. M. Hosseini, R. Simpson, and J. H. Park, "Myoelectric Control Systems for Upper Limb Wearable Robotic Exoskeletons and Exosuits—A Systematic Review," *Sensors*, vol. 22, no. 21, pp. 1–31, 2022, doi: 10.3390/s22218134.

[12] Y. Zhao *et al*., "Computationally Efficient Personalized EMG-Driven Musculoskeletal Model of Wrist Joint," in *IEEE Transactions on Instrumentation and Measurement*, vol. 72, pp. 1-10, 2023, doi: 10.1109/TIM.2022.3225023.

[13] M. Simao, N. Mendes, O. Gibaru, and P. Neto, "A Review on Electromyography Decoding and Pattern Recognition for Human-Machine Interaction," *IEEE Access*, vol. 7, no. c, pp. 39564–39582, 2019, doi: 10.1109/ACCESS.2019.2906584.

[14] L. Bi, A. Feleke, and C. Guan, "A review on EMG-based motor intention prediction of continuous human upper limb motion for human-robot collaboration," *Biomed. Signal Process. Control*, vol. 51, pp. 113–127, 2019, doi: 10.1016/j.bspc.2019.02.011.

[15] M. Gandolla *et al.*, "Artificial neural network EMG classifier for functional hand grasp movements prediction," *J. Int. Med. Res.*, vol. 45, no. 6, pp. 1831–1847, 2017, doi: 10.1177/0300060516656689.

[16] S. Zhang *et al.*, "Muscle strength assessment system using sEMG-based force prediction method for wrist joint," *J. Med. Biol. Eng.*, vol. 36, no. 1, pp. 121–131, 2016, doi: 10.1007/s40846-016-0112-5.

[17] Z. Lei, "An upper limb movement estimation from electromyography by using BP neural network," *Biomed. Signal Process. Control*, vol. 49, pp. 434–439, 2019, doi: 10.1016/j.bspc.2018.12.020.

[18] Y. Chen *et al.*, "A hierarchical dynamic Bayesian learning network for EMG-based early prediction of voluntary movement intention," *Sci. Rep.*, vol. 13, no. 1, p. 4730, 2023, doi: 10.1038/s41598-023-30716-7.

[19] D. Jiang, G. Li, Y. Sun, J. Kong, B. Tao, and D. Chen, "Grip strength forecast and rehabilitative guidance based on adaptive neural fuzzy inference system using sEMG," *Pers. Ubiquitous Comput.*, 2019, doi: 10.1007/s00779-019-01268-3.

[20] A. Phinyomark, F. Quaine, S. Charbonnier, C. Serviere, F. Tarpin-Bernard, and Y. Laurillau, "EMG feature evaluation for improving myoelectric pattern recognition robustness," *Expert Syst. Appl.*, vol. 40, no. 12, pp. 4832–4840, 2013, doi: 10.1016/j.eswa.2013.02.023.

[21] M. Atzori *et al.*, "Electromyography data for non-invasive naturally-controlled robotic hand prostheses," *Sci. Data*, vol. 1, pp. 1–13, 2014, doi: 10.1038/sdata.2014.53.

[22] R. N. Khushaba and S. Kodagoda, "Electromyogram (EMG) feature reduction using Mutual Components Analysis for multifunction prosthetic fingers control," *2012 12th International Conference on Control Automation Robotics & Vision (ICARCV)*, pp. 1534-1539, 2012, doi: 10.1109/ICARCV.2012.6485374.

[23] M. Atzori and H. Müller, "Control capabilities of myoelectric robotic prostheses by hand amputees: A scientific research and market overview," *Front. Syst. Neurosci.*, vol. 9, p. 162, 2015, doi: 10.3389/fnsys.2015.00162.

[24] M. Atzori, M. Cognolato, and H. Müller, "Deep learning with convolutional neural networks applied to electromyography data: A resource for the classification of movements for prosthetic hands," *Front. Neurorobot.*, vol. 10, pp. 1–11, 2016, doi: 10.3389/fnbot.2016.00009.

[25] L. Meng, J. Pang, Z. Wang, R. Xu, and D. Ming, "The role of surface electromyography in data fusion with inertial sensors to enhance locomotion recognition and prediction," *Sensors*, vol. 21, no. 18, 2021, doi: 10.3390/s21186291.

[26] B. Chen *et al.*, "Volitional control of upper-limb exoskeleton empowered by EMG sensors and machine learning computing," *Array*, vol. 17, p. 100277, 2023, doi: 10.1016/j.array.2023.100277.

[27] T. Kawase, T. Sakurada, Y. Koike, and K. Kansaku, "Estimating joint angles from biological signals for multi-joint exoskeletons," *2014 IEEE International Conference on Systems, Man, and Cybernetics (SMC)*, pp. 1470-1474, 2014, doi: 10.1109/SMC.2014.6974122.

[28] T. A. Kuiken, L. A. Miller, K. Turner, and L. J. Hargrove, "A Comparison of Pattern Recognition Control and Direct Control of a Multiple Degree-of-Freedom Transradial Prosthesis," in *IEEE Journal of Translational Engineering in Health and Medicine*, vol. 4, pp. 1-8, 2016, doi: 10.1109/JTEHM.2016.2616123.

[29] N. Jiang, S. Dosen, K. R. Muller, and D. Farina, "Myoelectric control of artificial limbsis there a need to change focus? [In the Spotlight]," *IEEE Signal Process. Mag.*, vol. 29, no. 5, pp. 148–152, 2012, doi: 10.1109/MSP.2012.2203480.

[30] Y. Zhao, Z. Li, Z. Zhang, K. Qian, and S. Xie, "An EMG-driven musculoskeletal model for estimation of wrist kinematics using mirrored bilateral movement," *Biomed. Signal Process. Control*, vol. 81, p. 104480, 2023, doi: 10.1016/j.bspc.2022.104480.

[31] M. R. Ahsan, M. I. Ibrahimy, and O. O. Khalifa, "Optimization of neural network for efficient EMG signal classification," *2012 8th International Symposium on Mechatronics and its Applications*, pp. 1-6, 2012, doi: 10.1109/ISMA.2012.6215165.

[32] E. Kilic and E. Dogan, "Design and fuzzy logic control of an active wrist orthosis," *Proc. Inst. Mech. Eng. Part H J. Eng. Med.*, vol. 231, no. 8, pp. 728–746, 2017, doi: 10.1177/0954411917705408.

[33] M. C. Tosin and A. Balbinot, "Identification and removal of contaminants in sEMG recordings through a methodology based on Fuzzy Inference and Actor-Critic Reinforcement learning," *Expert Syst. Appl.*, vol. 206, p. 117772, 2022, doi: 10.1016/j.eswa.2022.117772.

[34] M. Barfi, H. Karami, F. Faridi, Z. Sohrabi, and M. Hosseini, "Improving robotic hand control via adaptive Fuzzy-PI controller using classification of EMG signals," *Heliyon*, vol. 8, no. 12, 2022, doi: 10.1016/j.heliyon.2022.e11931.

[35] R. Suppiah, N. Kim, A. Sharma, and K. Abidi, "Fuzzy inference system (FIS) - long short-term memory (LSTM) network for electromyography (EMG) signal analysis," *Biomed. Phys. Eng. Express*, vol. 8, no. 6, 2022, doi: 10.1088/2057-1976/ac9e04.

[36] C. Garg, Y. Narayan, and L. Mathew, "Development of a software module for feature extraction and classification of EMG signals," *2015 Communication, Control and Intelligent Systems (CCIS)*, pp. 250-254, 2015, doi: 10.1109/CCIntelS.2015.7437917.

[37] M. Pang, S. Guo, and Z. Song, "Study on the sEMG driven Upper Limb Exoskeleton rehabilitation device in bilateral rehabilitation," *Journal of Robotics and Mechatronics*, vol. 24, no. 4. pp. 585–594, 2012, doi: 10.20965/jrm.2012.p0585.

[38] C. Loconsole *et al.*, "An emg-based robotic hand exoskeleton for bilateral training of grasp," *2013 World Haptics Conf. WHC 2013*, pp. 537–542, 2013, doi: 10.1109/WHC.2013.6548465.

[39] J. Ngeo *et al.*, "Control of an optimal finger exoskeleton based on continuous joint angle estimation from EMG signals," *Proc. Annu. Int. Conf. IEEE Eng. Med. Biol. Soc. EMBS*, pp. 338–341, 2013, doi: 10.1109/EMBC.2013.6609506.

[40] Z. Li, B. Wang, F. Sun, C. Yang, Q. Xie, and W. Zhang, "SEMG-based joint force control for an upper-limb power-assist exoskeleton robot," *IEEE J. Biomed. Heal. Informatics*, vol. 18, no. 3, pp. 1043–1050, 2014, doi: 10.1109/JBHI.2013.2286455.

[41] E. A. Kirchner, M. Tabie, and A. Seeland, "Multimodal movement prediction - Towards an individual assistance of patients," *PLoS One*, vol. 9, no. 1, 2014, doi: 10.1371/journal.pone.0085060.

[42] D. Leonardis *et al.*, "An EMG-controlled robotic hand exoskeleton for bilateral rehabilitation," *IEEE Trans. Haptics*, vol. 8, no. 2, pp. 140–151, 2015, doi: 10.1109/TOH.2015.2417570.

[43] A. Accogli *et al.*, "EMG-Based Detection of User's Intentions for Human-Machine Shared Control of an Assistive Upper-Limb Exoskeleton," *Wearable Robotics: Challenges and Trends: Proceedings of the 2nd International Symposium on Wearable Robotics, WeRob2016*, vol. 16, pp. 181–185, 2017, doi: 10.1007/978-3-319-46532-6.

[44] Z. Lu, X. Chen, X. Zhang, K. Y. Tong, and P. Zhou, "Real-Time Control of an Exoskeleton Hand Robot with Myoelectric Pattern Recognition," *Int. J. Neural Syst.*, vol. 27, no. 5, pp. 1–11, 2017, doi: 10.1142/S0129065717500095.

[45] Y. Yun *et al.*, "Maestro: An EMG-driven assistive hand exoskeleton for spinal cord injury patients," *Proc. - IEEE Int. Conf. Robot. Autom.*, pp. 2904–2910, 2017, doi: 10.1109/ICRA.2017.7989337.

[46] N. Irastorza-Landa *et al.*, "Design of continuous EMG classification approaches towards the control of a robotic exoskeleton in reaching movements," *IEEE Int. Conf. Rehabil. Robot.*, pp. 128–133, 2017, doi: 10.1109/ICORR.2017.8009234.

[47] H. Zeng, K. Li, N. Wei, R. Song, and X. Tian, "A sEMG-Controlled Robotic Hand Exoskeleton for Rehabilitation in Post-Stroke Individuals," *2018 IEEE Int. Conf. Cyborg Bionic Syst. CBS 2018*, pp. 652–655, 2019, doi: 10.1109/CBS.2018.8612211.

[48] M. Jana, B. G. Barua, and S. M. Hazarika, "Design and Development of a Finger Exoskeleton for Motor Rehabilitation using Electromyography Signals," *2019 23rd Int. Conf. Mechatronics Technol. ICMT 2019*, pp. 1–6, 2019, doi: 10.1109/ICMECT.2019.8932126.

[49] Z. Lu, A. Stampas, G. E. Francisco, and P. Zhou, "Offline and online myoelectric pattern recognition analysis and real-time control of a robotic hand after spinal cord injury," *J. Neural Eng.*, vol. 16, no. 3, 2019, doi: 10.1088/1741-2552/ab0cf0.

[50] N. Secciani, M. Bianchi, E. Meli, Y. Volpe, and A. Ridolfi, "A novel application of a surface ElectroMyoGraphy-based control strategy for a hand exoskeleton system: A single-case study," *Int. J. Adv. Robot. Syst.*, vol. 16, no. 1, pp. 1–13, 2019, doi: 10.1177/1729881419828197.

[51] M. K. Burns, D. Pei, and R. Vinjamuri, "Myoelectric control of a soft hand exoskeleton using kinematic synergies," *IEEE Trans. Biomed. Circuits Syst.*, vol. 13, no. 6, pp. 1351–1361, 2019, doi: 10.1109/TBCAS.2019.2950145.

[52] C. Dai and X. Hu, "Finger Joint Angle Estimation Based on Motoneuron Discharge Activities," *IEEE J. Biomed. Heal. Informatics*, vol. 24, no. 3, pp. 760–767, 2020, doi: 10.1109/JBHI.2019.2926307.

[53] Q. Zhang, T. Pi, R. Liu, and C. Xiong, "Simultaneous and Proportional Estimation of Multijoint Kinematics from EMG Signals for Myocontrol of Robotic Hands," *IEEE/ASME Trans. Mechatronics*, vol. 25, no. 4, pp. 1953–1960, 2020, doi: 10.1109/TMECH.2020.2999532.

[54] Y. Zhao, Z. Li, Z. Zhang, K. Qian, and S. Xie, "An EMG-driven musculoskeletal model for estimation of wrist kinematics using mirrored bilateral movement," *Biomed. Signal Process. Control*, vol. 81, p. 104480, 2023, doi: 10.1016/j.bspc.2022.104480.

[55] I. J. R. Martinez, A. Mannini, F. Clemente, and C. Cipriani, "Online Grasp Force Estimation from the Transient EMG," *IEEE Trans. Neural Syst. Rehabil. Eng.*, vol. 28, no. 10, pp. 2333–2341, 2020, doi: 10.1109/TNSRE.2020.3022587.

[56] T. Kapelner, M. Sartori, F. Negro, and D. Farina, "Neuro-Musculoskeletal Mapping for Man-Machine Interfacing," *Sci. Rep.*, vol. 10, no. 1, pp. 1–10, 2020, doi: 10.1038/s41598-020-62773-7.

[57] D. Piovesan and R. Bortoletto, "A geometrical approach to compute upper limb joint stiffness," *C. - Comput. Model. Eng. Sci.*, vol. 123, no. 1, pp. 23–47, 2020, doi: 10.32604/cmes.2020.09231.

[58] T. Cao, D. Liu, Q. Wang, O. Bai, and J. Sun, "Surface electromyography-based action recognition and manipulator control," *Appl. Sci.*, vol. 10, no. 17, 2020, doi: 10.3390/app10175823.

[59] L. Zhang, W. Qi, Y. Hu, and Y. Chen, "Disturbance-observer-based fuzzy control for a robot manipulator using an EMG-driven neuromusculoskeletal model," *Complexity*, vol. 2020, pp. 1-10, 2020, doi: 10.1155/2020/8814460.

[60] F. Xiao, L. Gu, W. Ma, Y. Zhu, Z. Zhang, and Y. Wang, "Real time motion intention recognition method with limited number of surface electromyography sensors for A 7-DOF hand/wrist rehabilitation exoskeleton," *Mechatronics*, vol. 79, p. 102642, 2021, doi: 10.1016/j.mechatronics.2021.102642.

[61] C. Xie, Q. Yang, Y. Huang, S. Su, T. Xu, and R. Song, "A Hybrid Arm-Hand Rehabilitation Robot with EMG-Based Admittance Controller," *IEEE Trans. Biomed. Circuits Syst.*, vol. 15, no. 6, pp. 1332–1342, 2021, doi: 10.1109/TBCAS.2021.3130090.

[62] M. M. Alam, A. A. Khan, and M. Farooq, "Effects of vibratory massage therapy on grip strength, endurance time and forearm muscle performance," *Work*, vol. 68, no. 3, pp. 619–632, 2021, doi: 10.3233/WOR-203397.

[63] D. A. Forman, G. N. Forman, and M. W. R. Holmes, "Wrist extensor muscle activity is less task-dependent than wrist flexor muscle activity while simultaneously performing moderate-to-high handgrip and wrist forces," *Ergonomics*, vol. 64, no. 12, pp. 1595–1605, 2021, doi: 10.1080/00140139.2021.1934564.

[64] N. Clautilde, R. Maxime, and A. Sofiane, "Impact of the choice of upper limb prosthesis mechanism on kinematics, and dynamic quality," *Med. Eng. Phys.*, vol. 94, pp. 16–25, 2021, doi: 10.1016/j.medengphy.2021.05.023.

[65] N. J. Chimera, M. W. R. Holmes, and D. A. Gabriel, "Anthropometrics and electromyography as predictors for maximal voluntary isometric wrist torque: Considerations for ergonomists," *Appl. Ergon.*, vol. 97, p. 103496, 2021, doi: 10.1016/j.apergo.2021.103496.

[66] C. Avian, S. W. Prakosa, M. Faisal, and J. S. Leu, "Estimating finger joint angles on surface EMG using Manifold Learning and Long Short-Term Memory with Attention mechanism," *Biomed. Signal Process. Control*, vol. 71, p. 103099, 2022, doi: 10.1016/j.bspc.2021.103099.

[67] S. Yang *et al*., "Learning-Based Motion-Intention Prediction for End-Point Control of Upper-Limb-Assistive Robots," *Sensors*, vol. 23, no. 6, p. 2998, 2023.

[68] Y. Bouteraa, I. Ben Abdallah, and K. Boukthir, "A New Wrist–Forearm Rehabilitation Protocol Integrating Human Biomechanics and SVM-Based Machine Learning for Muscle Fatigue Estimation," *Bioengineering*, vol. 10, no. 2, 2023, doi: 10.3390/bioengineering10020219.

[69] J. Li *et al.*, "Virtual regression-based myoelectric hand-wrist prosthesis control and electrode site selection using no force feedback," *Biomed. Signal Process. Control*, vol. 82, p. 104602, 2023, doi: 10.1016/j.bspc.2023.104602.

[70] M. S. Karis, H. A. Kasdirin, N. Abas, W. H. M. Saad and S. M. Aras, "EMG Based Control of Wrist Exoskeleton," vol. 24, no. 2, pp. 391–406, 2023, doi: 10.31436/iiumej.v24i2.2804.

[71] F. Xu, Y. Zheng, and X. Hu, "Estimation of Joint Kinematics and Fingertip Forces using Motoneuron Firing Activities: A Preliminary Report," 2021 *10th International IEEE/EMBS Conference on Neural Engineering (NER)*, pp. 1035-1038, 2021, doi: 10.1109/NER49283.2021.9441433.

[72] A. Prakash and S. Sharma, "A low-cost system to control prehension force of a custom-made myoelectric hand prosthesis," *Res. Biomed. Eng.*, vol. 36, no. 3, pp. 237–247, 2020, doi: 10.1007/s42600-020-00064-w.

[73] Y. Hu, Z. Li, G. Li, P. Yuan, C. Yang, and R. Song, "Development of Sensory-Motor Fusion-Based Manipulation and Grasping Control for a Robotic Hand-Eye System," *IEEE Trans. Syst. Man, Cybern. Syst.*, vol. 47, no. 7, pp. 1169–1180, 2017, doi: 10.1109/TSMC.2016.2560530.

[74] A. D. Sobel, K. N. Shah, and J. A. Katarincic, "The Imperative Nature of Physical Exam in Identifying Pediatric Scaphoid Fractures," *J. Pediatr.*, vol. 177, pp. 323-323, 2016, doi: 10.1016/j.jpeds.2016.06.086.

[75] V. Mendez, L. Pollina, F. Artoni, and S. Micera, "Deep Learning with Convolutional Neural Network for Proportional Control of Finger Movements from surface EMG Recordings," *2021 10th International IEEE/EMBS Conference on Neural Engineering (NER)*, pp. 1074-1078, 2021, doi: 10.1109/NER49283.2021.9441095.

[76] J. Lara, N. Paskaranandavadivel, and L. K. Cheng, "HD-EMG Electrode Count and Feature Selection Influence on Pattern-based Movement Classification Accuracy," *2020 42nd Annual International Conference of the IEEE Engineering in Medicine & Biology Society (EMBC)*, pp. 4787-4790, 2020, doi: 10.1109/EMBC44109.2020.9175210.

[77] A. Neacsu, J. -C. Pesquet, and C. Burileanu, "Accuracy-Robustness Trade-Off for Positively Weighted Neural Networks," *ICASSP 2020 - 2020 IEEE International Conference on Acoustics, Speech and Signal Processing (ICASSP)*, pp. 8389-8393, 2020, doi: 10.1109/ICASSP40776.2020.9053803.

[78] H. Hayashi, T. Shibanoki, and T. Tsuji, "A Neural Network Based on the Johnson SU Translation System and Related Application to Electromyogram Classification," *IEEE Access*, vol. 9, pp. 154304–154317, 2021, doi: 10.1109/ACCESS.2021.3126348.

[79] A. Subasi and S. M. Qaisar, "Surface EMG signal classification using TQWT, Bagging and Boosting for hand movement recognition," *J. Ambient Intell. Humaniz. Comput.*, vol. 13, no. 7, pp. 3539–3554, 2022, doi: 10.1007/s12652-020-01980-6.

[80] D. Copaci, D. Serrano, L. Moreno, and D. Blanco, "A high-level control algorithm based on sEMG signalling for an elbow joint SMA exoskeleton," *Sensors (Switzerland)*, vol. 18, no. 8, 2018, doi: 10.3390/s18082522.

[81] J. Schmidhuber, "Deep Learning in neural networks: An overview," *Neural Networks*, vol. 61, pp. 85–117, 2015, doi: 10.1016/j.neunet.2014.09.003.

[82] J. Huang, G. Li, H. Su, and Z. Li, "Development and Continuous Control of an Intelligent Upper-Limb Neuroprosthesis for Reach and Grasp Motions Using Biological Signals," *IEEE Trans. Syst. Man, Cybern. Syst.*, vol. 52, no. 6, pp. 3431–3441, 2022, doi: 10.1109/TSMC.2021.3069084.

[83] F. Pérez-Reynoso, N. Farrera, C. Capetillo, N. Méndez-Lozano, C. González-Gutiérrez, and E. López-Neri, "Pattern Recognition of EMG Signals by Machine Learning for the Control of a Manipulator Robot," *Sensors*, vol. 22, no. 9, 2022, doi: 10.3390/s22093424.

[84] P. Wojtczak, T. G. Amaral, O. P. Dias, A. Wolczowski, and M. Kurzynski, "Hand movement recognition based on biosignal analysis," *Eng. Appl. Artif. Intell.*, vol. 22, no. 4–5, pp. 608–615, 2009, doi: 10.1016/j.engappai.2008.12.004.

[85] F. N. Zohedi, M. S. M. Aras, H. A. Kasdirin, M. B. Bahar, M. K. Aripin, and F. A. Azis, "Modelling and controlling of Underwater Remotely Operated Vehicle vertical trajectory using Gradient Descent Algorithm Single Input Fuzzy Logic Controller and Fuzzy Logic Controller," *2022 IEEE 9th International Conference on Underwater System Technology: Theory and Applications (USYS)*, pp. 1-6, 2022, doi: 10.1109/USYS56283.2022.10072761.

[86] M. Karuna, C. Ganesh, R. P. Das, and M. V. Kumar, "Classification of wrist movements through EMG signals with fuzzy logic algorithm," *2017 International Conference on Energy, Communication, Data Analytics and Soft Computing (ICECDS)*, pp. 2258-2261, 2017, doi: 10.1109/ICECDS.2017.8389854.

[87] M. K. Tageldeen, N. Perumal, I. Elamvazuthi, and T. Ganesan, "Design and control of an upper arm exoskeleton using Fuzzy logic techniques," *2016 2nd IEEE International Symposium on Robotics and Manufacturing Automation (ROMA)*, pp. 1-6, 2016, doi: 10.1109/ROMA.2016.7847838.

[88] S. B. Joseph, E. G. Dada, A. Abidemi, D. O. Oyewola, and B. M. Khammas, "Metaheuristic algorithms for PID controller parameters tuning: review, approaches and open problems," *Heliyon*, vol. 8, no. 5, 2022, doi: 10.1016/j.heliyon.2022.e09399.

[89] G. Jia, H. K. Lam, J. Liao, and R. Wang, "Classification of electromyographic hand gesture signals using machine learning techniques," *Neurocomputing*, vol. 401, pp. 236–248, 2020, doi: 10.1016/j.neucom.2020.03.009.

[90] B. Bardizbanian *et al*., "Efficiently Training Two-DoF Hand-Wrist EMG-Force Models," *2020 42nd Annual International Conference of the IEEE Engineering in Medicine & Biology Society (EMBC)*, pp. 369-373, 2020, doi: 10.1109/EMBC44109.2020.9175675.